Energy Relaxation at a Hot-Electron Vortex Instability

James M. Knight* and Milind N. Kunchur†
Department of Physics and Astronomy, University of South Carolina, Columbia, SC 29208
(Dated: July 12, 2004)

Vortex motion in a superconducting film has been observed to become unstable at a critical vortex velocity v^*. At substrate temperatures substantially below T_c , the observed behavior can be accounted for by a model in which the electrons reach an elevated temperature relative to the phonons and the substrate. Here we examine the underlying assumptions concerning energy flow and relaxation times in this model. A calculation of the rate of energy transfer from the electron gas to the lattice finds that at the instability, the electronic temperature reaches a very high value close to the critical temperature. Our calculated energy relaxation times are consistent with those deduced from the experiments. We also estimate the phonon mean free path and its effect on the flow of energy, and show that the electronic thermal conductivity is sufficient to make the assumption of uniform electron temperature plausible.

PACS numbers: 71.10.Ca, 71.38.-k, 72.10.Di, 72.15.Lh, 73.50.Fq, 74.25.Fy, 74.72.Bk, 74.78.Bz

I. INTRODUCTION

When a film of a type II superconductor is placed in a magnetic field large enough to permit penetration of vortices, a transport current in the film acts on the vortices through a Lorentz force that is opposed by a pinning force and, eventually, by a drag force. When the Lorentz force exceeds the pinning force, the vortices are set into motion and the drag force comes into play. When the Lorentz force is substantially larger than the pinning forces but the transport current is still small compared to the depairing current, previous experiments[1–3] showed that the resulting dissipation is reasonably well described by the Bardeen-Stephen (BS) model[4]. In this region it is Ohmic, but as the current is increased, it becomes nonlinear and eventually reaches an instability manifested by a discontinuous increase in voltage. At temperatures not far below the critical temperature, the instability has been studied in a classic paper[5] by Larkin and Ovchinnikov (LO). They showed that the electron distribution departs from a thermal distribution at high vortex velocities, changing the superconducting order parameter and altering the drag force on the vortices. They predicted a non-linearity in the current-voltage characteristic and an instability in the vortex motion when the vortices reach a critical velocity v^*. The LO instability is due to a decrease in the drag force with increasing vortex velocity, accompanied by a decrease in vortex size. LO showed that the critical velocity is independent of the magnetic field. Early experiments on low-T_c systems[6] confirmed Larkin and Ovchinnikov's results and predictions. Subsequent experiments on $Y_1Ba_2Cu_3O_{7-\delta}$ (YBCO) by Doettinger, Huebener, Gerdemann, Kühle, Anders, Träuble, and Villègier[7] and by Xiao and Ziemann[8], also confirmed LO behavior.

However, experiments carried out at lower temperatures[9,10] on YBCO, showed a non-linearity and instability with a very different dependence of v^* on the magnetic field B. Analysis[9,10] showed that the new behavior could be accounted for by a simple model in which the electron gas has a thermal-like distribution function characterized by a higher temperature than the lattice and bath. Larkin and Ovchinnikov did, in fact, suggest this possibility in their original paper[11] without exploring its consequences. As the electron temperature rises, the resulting increase in resistivity causes a decrease in current above a certain electric field and hence a non-monotonic response. This model yields a critical vortex velocity v^* at instability that is proportional to $1/\sqrt{B}$, as seen in the low-T experiments. Some of the essential consequences of such a hot-electron instability were calculated in our earlier papers and shown to be consistent with experimental observations.

In the present work some of the simplifying assumptions and restrictions in the previous calculations have been removed and more complete calculations have been carried out:

(1) Previously we only considered vortex dissipation due to the BS mechanism; here we also include the Tinkham mechanism[12].

(2) The rate τ_ϵ^{-1} of transfer of energy from the electron gas to the lattice—which plays a crucial role in determining the electron temperature—was taken as a constant in previous discussions of the model. In this paper we show that it can be expected to have a strong temperature dependence. This temperature dependence of τ_ϵ is now included in our numerical calculations of the current-voltage curves. We find that the general shape of the current-voltage relation is not very sensitive to the temperature variation of τ_ϵ because the electron gas passes rapidly from the bath temperature to a temperature not far below T_c before any significant non-linearity is manifested. This is a consequence of the very small low-temperature specific heat of a superconducting electron gas. However, the strong temperature variation of the relaxation time gives a sensitive measure of the electron temperature. Evaluation of τ_ϵ from the data near the instability point indicates an electron temperature much higher than the bath temperature, supporting the heated electron picture of the instability. The calculation

of this electron-lattice energy relaxation time is presented in Section III below.

(3) Finally, if the film thickness is not negligible compared to the phonon mean free path—as was assumed in our previous work[9,10]—the phonons will not have a thermal distribution characterized by the bath temperature. In the present paper we take into account the effect of a finite phonon mean free path on the hot-electron vortex instability and consider the general situation where the phonons are not thermalized by the bath. Phonon lifetime effects can be taken into account following work by Bezuglij and Shklovsky[13], who solved the phonon kinetic equation for a thin film. The non-thermal phonon distribution found in this solution can be incorporated into our calculation of the energy transfer rate, and provides a correction to our earlier results. This result is derived in Section IV below.

We begin in Section II by giving a description of the model presenting some new numerical results on the current-voltage curves under various conditions and critical parameters at the instability.

II. MODEL FOR INSTABILITY

The macroscopic fields in a type II superconductor carrying a transport current are related to the velocity of the vortices by the fundamental relation

$$v = \frac{E}{B}c, \tag{1}$$

which follows from the law of induction. This equation can be used to find the electric field once the vortex velocity is determined by considering the fundamental dissipative processes in the medium. Elastic forces can be shown to be negligible. One of the dissipative processes is the scattering of normal electrons in the vortex core and quasiparticles outside the core first treated by Bardeen and Stephen. They found that the transport current density j is expressed in terms of the upper critical field H_{c2} and the normal resistivity ρ_n by

$$j_1 = \frac{H_{c2}}{\rho_n}\frac{v}{c} = \frac{H_{c2}}{\rho_n}\frac{E}{B}. \tag{2}$$

More elaborate treatments[14] give results that agree with Eq.(2) to within a numerical factor of order 1. Another contribution to the dissipation arises from the non-equilibrium conditions that exist on the leading and trailing side of the moving vortex because of the finite relaxation time of the order parameter. This mechanism was first treated by Tinkham, who gave an expression equivalent to the following for the transport current density in terms of the order parameter relaxation time τ_Δ and the zero-field zero-temperature gap Δ_{00}:

$$j_2 = \frac{gH_{c2}}{\rho_n B}E, \tag{3}$$

where

$$g = \frac{a\hbar}{\Delta_{00}\tau_\Delta}\,(1-t^4), \tag{4}$$

and $t = (T/T_c)$, and a is a numerical coefficient of order unity. This has the same order of magnitude as Eq.(2) but a somewhat different temperature dependence. The resistivities implied by these two contributions to the dissipation are additive, yielding the total current

$$j = \frac{g}{g+1}\frac{H_{c2}}{\rho_n B}E. \tag{5}$$

These energy dissipation mechanisms raise the energy of the electrons, and this energy subsequently relaxes to the lattice. The assumption of the model is that the electron-electron scattering time is small enough compared to the electron-phonon inelastic scattering time that the electron gas remains in internal thermal equilibrium at a temperature higher than the lattice temperature. While a full justification is beyond the scope of this paper the plausibility of the assumption can be checked by estimating the cross-over temperature below which electron-electron scattering is dominant. The standard estimates[15] of the scattering rates $\tau_{ee}^{-1} = \eta\epsilon_F/T^2$ and of $\tau_{ep}^{-1} = \eta^3\omega_D^2/T^3$ then give a cross-over temperature of the order of 100 K for parameters appropriate to YBCO. This temperature is indeed higher than the range of interest in the experiments.

Changes in the energy density of the electron gas can be described by a rate equation that includes the work done by the electric field and the exchange of energy with the lattice. If we assume that the exchange can be described approximately by an energy relaxation time τ_ϵ , then the equation is

$$\frac{du}{dt} = jE - \frac{u(T') - u(T_p)}{\tau_\epsilon(T', T_p)}, \tag{6}$$

where τ_ϵ can depend on the temperature T_p of the phonons as well as the electron temperature T'. We argue below that the dependence of τ_ϵ on T_p is weak enough to be ignored in the relevant range of temperatures and the relevant energy transfer rates between the lattice and the bath. The quasiparticles transfer the energy they receive from the transport current to the lattice at a rate much higher than it is radiated back, and the energy then flows from the lattice to the bath. Thus τ_ϵ can be assumed to depend only on T', and we can write the steady-state equation

$$jE\tau_\epsilon = \int_{T_p}^{T'} c(T)dT, \tag{7}$$

where the energy difference in Eq.(6) has been expressed in terms of the electronic specific heat per unit volume.

Equations (2) - (7) determine the relationship between the electric field, the current density and the temperature. The temperature dependence of the specific heat

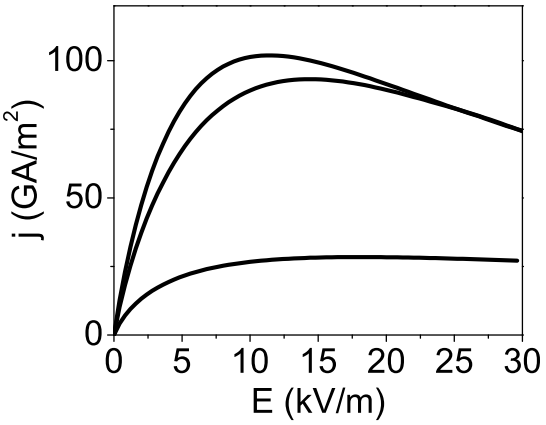

FIG. 1: Current density vs electric field for $B = 8$ Tesla. Upper curve: Bardeen Stephen model with a constant τ_ϵ . Middle curve: Bardeen Stephen model with a τ_ϵ varying with T according the calculation in the text. Lower curve: Bardeen Stephen model with Tinkham mechanism added and with a variable τ_ϵ . The value of τ_ϵ used in the fixed τ_ϵ curve corresponds to the calculated value near T_c.

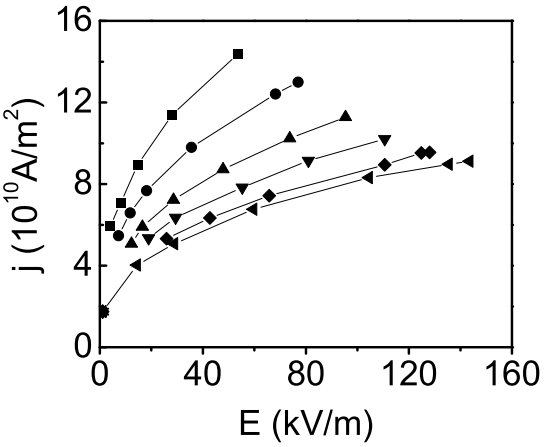

FIG. 2: Experimental curves of current density vs electric field in YBCO for flux density (beginning with the upper curve) $B = 3$, 5, 8, 11, 14, and 16 Tesla.

and the upper critical field are taken from standard BCS theory[16]. In calculating the specific heat, the temperature dependence of the gap was taken from BCS theory and its magnitude was multiplied by a factor to give the observed zero-temperature gap[17] and critical temperature. The temperature dependence of the order parameter relaxation time is determined empirically as suggested by Tinkham[12]. The energy relaxation time and its temperature dependence used in this section is calculated in the next section.

Typical results of the model are presented in the following figures. Fig. 1 shows the effects of the temperature variation of τ_ϵ and of inclusion of the Tinkham dissipation mechanism in addition to the Bardeen-Stephen mechanism. These are to be compared to the experimental data shown in Fig. 2. There is general qualitative agreement in the rising portion of the curve showing decreasing differential conductivity. While the value of the peak current reached is in general agreement with the model, the value E^* of E at which the peak in j is reached is an order of magnitude greater than the predicted value. This value is in somewhat better agreement when Tinkham dissipation is included, although the peak current is then a factor of five below the observed value. In assessing the comparison of experimental data with the model, it should be noted that there are no adjustable parameters in the calculation of τ_ϵ , which was done with simple assumptions about the strength of the electron-phonon interaction (Section below). We therefore conclude that the agreement is within acceptable bounds.

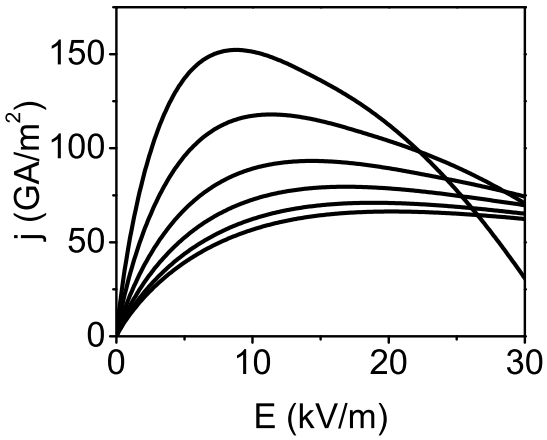

FIG. 3: Effect of increasing flux density on the current density vs electric field curve calculated in the model with variable τ_ϵ . Values of B beginning at the upper curve are 3, 5, 8, 11, 14, and 16 Tesla.

The onset of the unstable region in the current-voltage response does not require explicitly invoking the forces on the vortices in treatment of the model. Rather, the instability appears in the result as a region of negative differential conductivity, where j decreases as a function of E. The region begins at the value E^* of the field that can be determined by calculating dj/dE from Eq.(7), setting the result equal to zero, and solving for E:

$$E^* = \sqrt{\frac{C\rho_n B}{gH_{c2}\tau_\epsilon' + (gH_{c2})'\tau_\epsilon)}}, \tag{8}$$

where primes indicate differentiation with respect to temperature.[28] The experimentally well-verified $\sqrt{B}$ dependence of the electric field at instability follows provided the temperature T^* at this point is independent

or weakly dependent on B so that the temperature-dependent factors C, τ_ϵ , g, and H_{c2} in Eq.(8) remain independent of B. This result is a consequence of our model, since we have explicitly excluded a field dependence for these quantities and taken ρ_n to be temperature and field independent. Although Volovik[18] has shown that the specific heat has a B-dependence in type II materials above the lower critical field, we have checked that his scaling prediction at low temperatures gives only a weak dependence in the range of fields $B << H_{c2}$ relevant to our experiment. Fig. 3 shows the calculated magnetic field dependence of the current vs voltage curve.

Fig. 4 shows the change in the electron temperature as a function of the applied electric field. The rise in temperature and corresponding decrease in H_{c2} result in decreasing differential conductivity which leads to the instability. Fig. 5 shows the relatively small effect of increasing bath temperature, up to about 50K, on the final temperature reached by the electron gas. The circles show the calculated T' at the instability peak (maxima in the curves of Fig. 3) and the crosses show the T' at one fixed value of applied electric field.

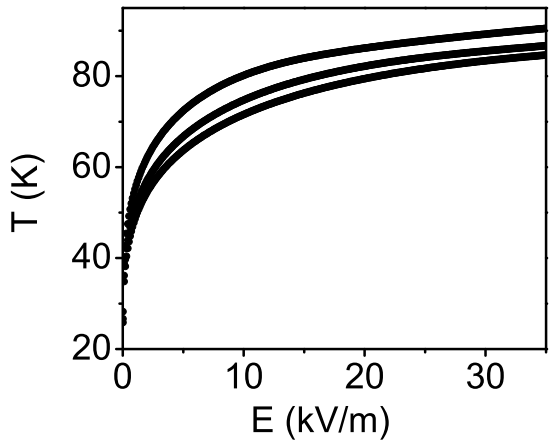

FIG. 4: Calculated electron temperature T' vs electric field E for $B = 3, 8,$ and16 Tesla.

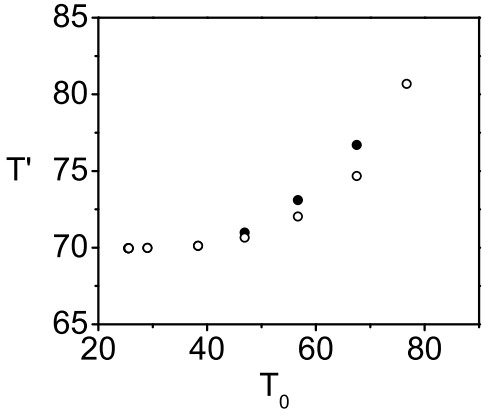

FIG. 5: Calculated electron temperature T^* at the peak of the current-voltage curve (solid circles) and at $E = 35$kV/m (open circles) for different phonon temperatures T_p

III. ENERGY TRANSFER RATE

The total rate at which energy is radiated by the heated quasiparticle gas to the lattice can be calculated by standard methods[19,20]. The two contributing processes, phonon emission and quasiparticle recombination with emission of a phonon, are illustrated schematically in Fig. 6. Taking into account the isotropy of the rate

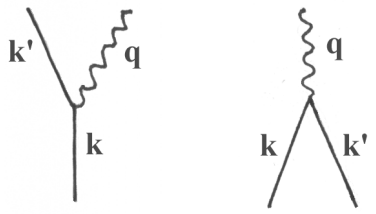

FIG. 6: Diagrams contributing to the energy transfer rate from the quasiparticle gas to the lattice.

with respect to the initial electron momentum, the result for phonon emission is:

$$P_e = \frac{16\pi^2}{\hbar}\left(\frac{V}{(2\pi)^3}\right)^2 \int\int\int k^2 dk k^{'2} dk^{'} d\Omega_{k'} |\mathcal{M}_{\mathbf{k}-\mathbf{k}'}|^2 f_e(E,E^{'})\delta(E-E^{'}-\hbar s|\mathbf{k}-\mathbf{k}^{'}|)\hbar s|\mathbf{k}-\mathbf{k}^{'}| \quad (9)$$

$$= \frac{2Vm^2}{\pi\hbar^3}\int\int\int d\omega d\epsilon d\epsilon^{'} v_F \alpha^2(\omega)F(\omega)\hbar\omega f_e(E,E^{'})\delta(E-E^{'}-\hbar\omega). \quad (10)$$

where the coherence factor and occupation factors have been combined in the function

$$f_e(E,E^{'}) = \frac{f(E_{\mathbf{k}})(1-f(E^{'}_{\mathbf{k}})}{1-f(E_{\mathbf{k}})}\left(1-\frac{\Delta_{\mathbf{k}}\Delta_{\mathbf{k}'}}{E_{\mathbf{k}}E_{\mathbf{k}'}}\right). \quad (11)$$

In the second form of P_e, we have changed from momentum variables to bare electron energy variables and introduced the dimensionless electron-phonon spectral function $\alpha^2 F$, defined by:

$$\alpha^2(\omega)F(\omega) = \frac{V}{(2\pi)^3\hbar^2}\int \frac{d^2k^{'}}{v^{'}_F}|\mathcal{M}_{\mathbf{k}-\mathbf{k}'}|^2\delta(\omega - s|\mathbf{k}-\mathbf{k}^{'}|). \quad (12)$$

In the deformation potential approximation[21] where

$$|\mathcal{M}_{\mathbf{k}-\mathbf{k}'}|^2 = \frac{\hbar|\mathbf{k}-\mathbf{k}^{'}|}{2\rho s V}\left(\frac{2\epsilon_F}{3}\right)^2, \quad (13)$$

$\alpha^2(\omega)F(\omega)$ is of the form $b\omega^2$, where

$$b = \frac{m}{8\pi^2\hbar^2\rho s^4 k_F}\left(\frac{2\epsilon_F}{3}\right)^2. \quad (14)$$

Introducing this form of $\alpha^2(\omega)F(\omega)$ and changing from the bare electron energy ϵ to the quasiparticle energy E, the rates for phonon emission and quasiparticle recombination can be brought into the simple form

$$P_e = V\Sigma_e(T)(T/T_c)^5, \quad (15)$$

$$P_r = V\Sigma_r(T)(T/T_c)^5, \quad (16)$$

where

$$\Sigma_e(T) = A\int_z^\infty dx \int_0^{x-z} dy y^3 f_e(x,x-y)N(x-y,z)N(x,z), \quad (17)$$

$$\Sigma_r(T) = A\int_z^\infty dx \int_{x+z}^\infty dy y^3 f_r(x,y-x)N(y-x,z)N(x,z). \quad (18)$$

Here z is $\Delta(T)/T$, and $N(x,z)$ is the dimensionless quasiparticle density of states $\mathrm{Re}(x/\sqrt{x^2-z^2})$. The value of the constant A is $8m^2T_c^5 v_F b/(\pi\hbar^6)$. The temperature dependence of Σ_e and Σ_r comes from the temperature dependence of the gap through the parameter z. This modifies the simple T^5 dependence found in Wellstood, Urbina, and Clarke[20] for the transfer rate in normal metals and gives a much stronger dependence in the superconducting system.

The rates due to emission and recombination have been calculated numerically from the above equations. The net rate can be equated to $(u(T)-u(T_p))/\tau_\epsilon$ according to Eq.6 and the energy relaxation rate can be found as a function of temperature. The results are given in Fig. 7. Fig. 8 shows the energy relaxation time τ_ϵ found by equating the total transfer rate from emission and recombination to the last term in the rate equation 6.

Experimental values of τ_ϵ can be extracted from the data on the basis of the model and compared with the calculated times from this section. In the comparison shown in Fig. 9, τ_ϵ was determined in the vicinity of the peak in the current-field curve (at E^*) for various lattice temperatures T_p. The value at the peak is appropriate for a comparison because the shape of the curve is insensitive to the value of τ_ϵ at lower temperatures because of the rapid heating of the electrons at these temperatures. The agreement in order of magnitude of the measured and calculated values can be taken as an indication that the electron temperature is high, in view of the strong T dependence of τ_ϵ shown in Fig. 8. The rapid variation of τ_ϵ with temperature serves as a sensitive temperature indicator, showing that the electron temperature is indeed near T_c .

We note the following properties of the energy transfer rate:

1.) The rate of energy transfer from the electrons to the lattice at any given temperature is equal to the rate of transfer from the lattice to the electrons at the same temperature. Indeed, the rate from phonon emission balances the rate from absorption and the rate from quasiparticle recombination balances the rate from pair creation. These results can be demonstrated in the deformation potential approximation, where the matrix element for phonon emission and absorption depends only

on the phonon energy ν. For example, the rates for emission and absorption and for quasiparticle recombination and creation can be written

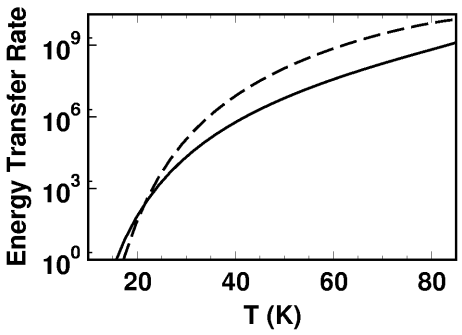

FIG. 7: Calculated energy transfer rate in meV/nm^3-s of electron gas at temperature T to a zero temperature lattice. The solid curve represents the phonon emission process and the dashed curve represents the quasiparticle annihilation process.

$$
\begin{aligned}
P_e &= G\int (n(\nu)+1) f_e(E, E-\nu) N(E) N(\nu - E) \nu^3 dE d\nu \\
P_a &= G\int n(\nu) f_a(E, E+\nu) N(E) N(E+\nu) \nu^3 dE d\nu, \\
P_r &= G\int (n(\nu)+1) f_r(E, \nu-E) N(E) N(\nu - E) \nu^3 dE d\nu \\
P_c &= G\int n(\nu) f_c(E, \nu-E) N(E) N(\nu - E) \nu^3 dE d\nu,
\end{aligned}
$$

where $n(\nu)$ is the phonon occupation number at the given temperature and $N(E)$ is the quasiparticle density of states, and G has the value $8Vm^3v_F b/\pi\hbar^6$. The equality of the rates is evident upon substituting the explicit forms of the Fermi and Bose distribution functions. In the same manner, the emission and absorption rates are identical after the same substitutions and the change of variable $E^{'} = E + \nu$ in P_a.

2.) The differences between the emission and absorption rates and the between the pair recombination and creation rates have only a weak dependence on the lattice temperature as long as the electron temperature is near T_c and the lattice temperature is low, say $T_p \leq T_c/2$. This conclusion is based on values for T_c (7.8 meV) and Δ (19 meV) for YBCO. Wellstood, Urbina, and Clarke,[20], assert that the difference between the emission rate and the absorption rate for a normal metal is equal to the difference between the rate electrons radiate to a zero temperature lattice and rate phonons radiate to a zero temperature electron gas. This result is only approximately valid in the gas of quasiparticles. The differences can be calculated from the previous pairs of equations by taking $n(\nu)$ to be the phonon distribution function at T_p. The difference between emission and absorbtion rates, for example, is:

$$P_e - P_a = G\int_{\Delta}^{\infty} dE \int_0^{E-\Delta} d\nu f_e(E, E-\nu) \frac{e^{\nu/T_p} - e^{\nu/T'}}{e^{\nu/T_p} - 1}.$$

The dependence on T_p is contained in the last factor. For ν of the order of Δ, T' of the order T_c, and T_0 in the range zero to $T_c/2$, this factor only varies from 1.0 to 0.915, showing therefore a weak dependence of the difference on T_p. In fact, the differences have been calculated explicitly for $T = 0.8\ T_c$ and T_p ranging from $0.1\ T_c$ to $0.5\ T_c$. The difference varies less than 10% for emission and absorbtion and less than 1% for the dominant creation and recombination. In view of these results, we

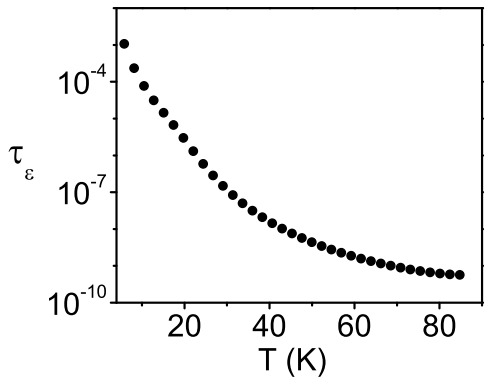

FIG. 8: Energy relaxation time τ_ϵ as a function of temperature.

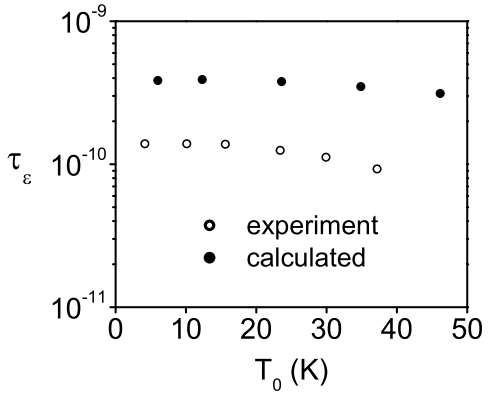

FIG. 9: Values of τ_ϵ extracted from the data on the basis of our model compared to values calculated in this section. General agreement in order of magnitude indicates an electron temperature near T_c.

ignore the dependence on T_p and calculate τ_ϵ on the basis of the radiation rate to a zero temperature lattice. A very similar argument applies to the difference between the pair recombination and pair creation rates.

3.) Quasiparticle emission and absorbtion can only satisfy the energy and momentum conservation laws if the the quasiparticle velocity $v_F \partial E/\partial \epsilon$ before emission or after absorbtion is greater than the sound velocity. This Čerenkov condition should be taken into account in the averaging near the Fermi surface that enters into calculation of the electron-phonon spectral function $\alpha^2 F$. In the integrals over quasiparticle energy above, the lower limit should be the energy E_c at which quasiparticles reach the sound velocity rather than Δ. The correction is of the order of the square of the ratio of the sound velocity to the Fermi velocity. Since $s/v_F << 1$ for all superconductors ($s/v_F \approx 1.5 \times 10^{-2}$ in YBCO), the correction can be safely ignored.

We should remark at this point that the calculations assumed an *s*-wave symmetry of the order parameter rather than the *d*-wave symmetry now well established for YBCO. However, this is not expected to have a serious influence on the qualitative value of the results, since the specific heats are qualitatively similar and the energy transfer rates are expected to be similar. The results presented would apply to the low-temperature type II *s*-wave superconductors, but these have not been explored to date because of the novelty of the technique. The quantitative determination of τ_ϵ in YBCO from the experimental data would be improved by a treatment taking account of the *d*-wave symmetry of the order parameter.

IV. PHONON LIFETIME EFFECTS

In the above discussion, we have not distinguished the phonon temperature and the bath temperature. We now consider corrections arising from a more general treatment of the phonon distribution. The standard estimate of phonon mean free path for normal metals $\hbar v_F/kT$ gives 17 nm when the Fermi velocity is taken to be 2×10^5 m/s, which is considerably shorter than the 100 nm thickness of the experimental films. The estimate of Kaplan, Chu, Langenberg, Chang, Jafarey, and Scalapino[19] of quasiparticle and phonon lifetimes in an *s*-wave superconductor below the critical temperature gives a frequency- and temperature-dependent numerical factor of order unity multiplied by the characteristic time

$$\tau_0^{ph} = \frac{\hbar N \langle \alpha^2 \rangle_{av}}{4\pi^2 N(0)} \Delta(0), \tag{19}$$

where N is the ion number density, $\langle \alpha^2 \rangle_{av}$ is the average electron-phonon coupling constant, $N(0)$ is the single-spin electronic density of states at the Fermi surface, and $\Delta(0)$ is the zero-temperature gap. Taking[22] the values $N = 13$ per unit cell, $\langle \alpha^2 \rangle_{av} = 5$ meV, $N(0)$ calculated from the free-electron theory with v_F having the value quoted above, and $\Delta(0) = 19$ meV, and converting the lifetime to a mean free path using the longitudinal sound velocity 4.2×10^3 m/s yields a path of the order of 10^3 nm, an order of magnitude larger than the thickness of the experimental film.

These estimates indicate that we are dealing with a marginal case where the phonon mean free path could be comparable to the thickness of the sample. To deal with the general case, we follow Bezuglij and Shklovskij[13], writing the kinetic equation for the phonon distribution function $n(\mathbf{q}, z)$ as

$$s_z \frac{\partial n(\mathbf{q}, z)}{\partial z} = -\frac{n(\mathbf{q}, z) - n(T)}{\tau_{ph}}, \tag{20}$$

where s_z is the component of the sound velocity perpendicular to the plane of the film and $n(T)$ is the thermal phonon distribution at the electron temperature. If phonons are reflected at the free surface of the film and

transmitted with average coefficient α at the substrate interface, it is found that the phonon distribution function is a linear combination of two thermal distributions, one at the bath temperature and one at the electron temperature. The coefficients in the linear combination depend on the position within the film and on the direction of propagation of the phonons:

$$n = A(z,\theta)n(T) + B(z,\theta)n(T_0). \tag{21}$$

The integrand in the expression for the energy transfer rate from quasiparticle gas to lattice contains the factor $n+1$, while that for the reverse rate contains a factor n. If Eq.(21) is substituted into these rates and account is taken of the condition for equilibrium between the lattice and the gas, the resulting rate contains a term with the factor $1-A$ and a term with the factor $Bn(T_0)$. For purposes of estimating the correction for finite phonon lifetime, we neglect the term proportional to $n(T_0)$ compared to the $1-A$ term on the ground that the phonon number is small at a temperature T_0 which is much smaller than the Debye temperature. An estimate of the remaining term can be obtained by replacing $1-A$ in the integral for the rate by its average value over the thickness of the film and over the directions of propagation of the phonon. The remaining integral is the one we evaluated in the previous section.

d/l	$\alpha = 0.8$	$\alpha = 0.5$	$\alpha = 0.2$
6.0	0.0333	0.0208	0.00833
1.0	0.190	0.121	0.0493
0.1	0.680	0.553	0.325

TABLE I: Calculated values of the phonon lifetime factor $1-A$ for three values of the ratio of thickness d to phonon mean free path l and three values of the average transmission coefficient α.

The explicit expression for A

$$A = 1 - \frac{\alpha}{1-(1-\alpha)e^{-2d/l_z}} \left\{ \begin{array}{ll} e^{-z/l_z} & , \ q_z > 0 \\ e^{-(2d-z)/l_z} & , \ q_z < 0 \end{array} \right\} \tag{22}$$

reflects the gradual change of the distribution (21) from a nearly thermal distribution at the bath temperature at the substrate interface $z=0$ to an electron temperature thermal distribution over the distance of a phonon mean free path. The transmission probability α can be determined in principle[23] from the measured value of the thermal resistance of the film-substrate interface, defined as the ratio of ΔT at the interface to the product of the power dissipated per unit volume and the thickness of the film. The measured value for YBCO is given by Nahum[24,25] as 1×10^{-3} Kcm^2/W. The determination of α is affected by uncertainties due to the averaging and due to the sensitive temperature variation of the thermal resistance. A literal application of Eq.[14] of reference[23] produces the average value 0.184 when d is of the order of or larger than l. When $d \ll l$, Shklovskii shows that the effective α is $2d/l$, which is 0.2 for the longest estimate of phonon mean free path above. We therefore accept 0.2 as a reasonable value. Sensitivity of the value of $1-A$ to d/l and α are shown in Table I. The longest estimate of phonon mean free path with the best estimate of the transmission coefficient indicate that the energy transfer rate will be multiplied by a factor of 0.325 due to phonon lifetime effects.

V. CONCLUSION

The electromagnetic behavior of YBCO films at high electric fields and current densities can be accounted for by a simple heating model in which the elevated temperature due to dissipation and the consequent changes in the properties of the electron gas result in an instability in the motion of vortices at which the differential conductivity vanishes. The work presented here justifies such a model by showing that the temperature variation of the energy transfer rate between the lattice and the electrons is consistent with the observed behavior, and that if the phonon mean free path is not too small compared to the film thickness, the necessary temperature difference between electrons and lattice can be maintained. The observed instability is a consequence.

VI. ACKNOWLEDGEMENTS

We thank B. I. Ivlev for important suggestions, and M. Geller, R. P. Huebener, and R. P. Prozorov for helpful discussions and criticisms. This work was supported by the U. S. Department of Energy through grant number DE-FG02-99ER45763.

* Electronic address: knight@sc.edu
† Electronic address: kunchur@sc.edu; URL: http://www.physics.sc.edu/kunchur

[1] M. N. Kunchur, D. K. Christen, and J. M. Phillips, Phys. Rev. Lett. **70**, 998 (1993);
[2] M. N. Kunchur, D. K. Christen, C. E. Klabunde, and J. M. Phillips, Phys. Rev. Lett. 72, 2259 (1994).
[3] M. N. Kunchur, B. I. Ivlev, D. K. Christen, and J. M. Phillips, Phys. Rev. Lett. **84**, 5204 (2000).
[4] J. Bardeen and M.J. Stephen, Phys. Rev. **140**, A1197 (1965).
[5] A. I. Larkin and Yu. N. Ovchinnikov, in *Nonequilibrium Superconductivity*, D. N. Langenberg and A. I. Larkin, eds. (Elsevier, Amsterdam 1986), Chapter 11.
[6] W. Klein, R. P. Huebener, S. Gauss, and J. Parisi, J. Low Temp. Phys. **61**, 413 (1985); and L. E. Musienko, I. M.

Dmitrenko, and V. G. Volotskaya, Pis'ma Zh. Eksp.Teor. Fiz. **31**, 603 (1980) [JETP Lett. **31**, 567 (1980)].

[7] S. G. Doettinger, R. P. Huebener, R. Gerdemann, A. Kühle, S. Anders, T. G. Träuble, and J. C. Villègier, Phys. Rev. Lett. **73**, 1691 (1994).

[8] Z. L. Xiao and P. Ziemann, Phys. Rev. B **53**, 15265, (1996).

[9] M. N. Kunchur, Phys. Rev. Lett. **89**, 137005 (2002).

[10] M. N. Kunchur and J. M. Knight, Mod. Phys. Lett. B **17**, 549 (2003).

[11] A. I. Larkin and Yu. N. Ovchinnikov, Zh. Eksp. Teor. Fiz. **68**, 1915 (1975)[Sov Phys. JETP **41**, 960 (1976)].

[12] M. Tinkham, Phys. Rev. Lett. **13**, 804 (1964).

[13] A. I. Bezuglij and V. A. Shklovskij, Physica C, **202**, 234 (1992).

[14] A. I. Larkin and Yu. N. Ovchinnikov, in *Nonequilibrium Superconductivity* eds. D. N. Langenberg and A. I. Larkin (Elsevier, Amsterdam, 1986), Chap. 11; C. R. Hu and R. S. Thompson, Phys. Rev. **B6**, 110 (1972); R. S. Thompson and C. R. Hu, Phys. Rev. Lett. **27**, 1352 (1971).

[15] A. Abrikosov, *Fundamentals of the Theory of Metals* (North Holland, Amsterdam 1988).

[16] N. R. Werthamer, E. Helfand, and P. C. Hohenberg, Phys. Rev **147**, 295, (1966).

[17] Wang Lanping, He Jian, and Wang Guowen., Phys. Rev. B **40**, 10954 (1989); and R. T. Collins, Z. Schlesinger, R. H. Koch, R. B. Laibowitz, T. S. Plaskett, P. Freitas, W. J. Gallagher, R. L. Sandstrom, and T. R. Dinger, Phys. Rev. Lett. **59**, 704 (1987).

[18] G. E. Volovik, Pis'ma Zh. Eksp. Teor. Fiz. **65**, 465 (1997) [JETP Lett. **65**, 491 (1997)].

[19] S. B. Kaplan, C. C. Chu, D. N.Langenberg, J. J. Chang, S. Jafarey,and D. J. Scalapino, Phys. Rev. B **14**, 4854 (1976).

[20] F. C. Wellstood, C. Urbina, and John Clarke, Phys. Rev. B **49**, 5942 (1994).

[21] J. M. Ziman, *Principles of the Theory of Solids* (Cambridge University Press, Cambridge, 1979).

[22] NIST WebHTS Database, http://www.ceramics.nist.gov/srd/hts/ htsquery.htm

[23] V. A. Shklovskii, Zh. Eksp. Teor. Fiz. **78**, 1281 (1980) [Sov. Phys. JETP **51**, 646 (1980)].

[24] M. Nahum, S. Verghese, P. L. Richards, and K. Char, Appl. Phys. Lett. **59**, 2034 (1991).

[25] M. L. Kunchur, Mod. Phys. Lett. B **9**, 299 (1995).

[26] M. N. Kunchur, B.I. Ivlev, and J. M. Knight, Phys. Rev. Lett. **87**, 177001 (2001).

[27] M. N. Kunchur, B.I. Ivlev, and J. M. Knight, Phys. Rev. B **66**, 060505 (2002).

[28] A secondary consequence of this instability is a fragmentation of the flux flow in the region of negative dj/dE resulting in steps in the current-voltage curves. Such steps have been observed in constant-voltage measurements at high dissipations[26,27].